

Clare Peters-Libeu,<sup>a</sup> Yvonne Newhouse,<sup>a</sup> Preethi Krishnan,<sup>a</sup> Kenneth Cheung,<sup>a</sup> Elizabeth Brooks,<sup>a</sup> Karl Weisgraber<sup>a,b</sup> and Steven Finkbeiner<sup>a,c\*</sup>

<sup>a</sup>Gladstone Institute of Neurological Disease, 1650 Owens Street, San Francisco, CA 94158, USA, <sup>b</sup>Department of Pathology, University of California, San Francisco, CA 94143, USA, and <sup>c</sup>Departments of Neurology, Physiology and Neuroscience and Biomedical Sciences Program, University of California, San Francisco, CA 94143, USA

Correspondence e-mail: sfinkbeiner@gladstone.ucsf.edu

Received 12 August 2005  
Accepted 8 November 2005  
Online 24 November 2005

## Crystallization and diffraction properties of the Fab fragment of 3B5H10, an antibody specific for disease-causing polyglutamine stretches

Because it binds soluble forms of proteins with disease-associated polyglutamine expansions, the antibody 3B5H10 is a powerful tool for studying polyglutamine-related diseases. Crystals of the 3B5H10 Fab (47 kDa) were obtained by vapor diffusion at room temperature from PEG 3350. However, the initial crystals gave highly anisotropic diffraction patterns. After optimization of the crystallization conditions and cryoprotectants, a nearly isotropic diffraction pattern at 2.6 Å resolution was achieved for crystals with unit-cell parameters  $a = 133.26$ ,  $b = 79.52$ ,  $c = 41.49$  Å and space group  $P2_12_12$ . Dehydrated crystals diffracted isotropically to 1.9 Å with unit-cell parameters  $a = 123.65$ ,  $b = 78.25$ ,  $c = 42.26$  Å,  $\beta = 90.3^\circ$  and space group  $P2_1$ .

### 1. Introduction

Homomeric polyglutamine (polyQ) expansions in nine distinct proteins are the only common denominator among a family of neurodegenerative disorders that includes Huntington's disease (HD; Zoghbi & Orr, 2000). HD occurs when the polyQ stretch exceeds a critical length (~36–40 glutamines) in the protein huntingtin (MacDonald, 1998). Above that threshold, the age of disease onset is inversely related to polyQ length. Similar thresholds exist for most other diseases associated with polyQ expansions. The molecular basis for the disease threshold or for the inverse relationship between neurodegeneration and polyQ length is unknown.

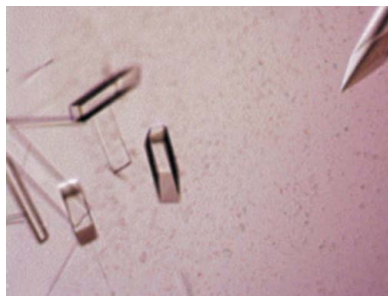
Abnormal polyQ expansions render proteins prone to aggregation (Scherzinger *et al.*, 1999). Highly aggregated forms of mutant huntingtin called inclusion bodies were initially thought to cause HD (Davies *et al.*, 1997). However, recent studies have suggested that less aggregated or possibly unaggregated forms of mutant huntingtin may be neurotoxic (Arrasate *et al.*, 2004; Klement *et al.*, 1998; Saudou *et al.*, 1998). These observations led to the proposal that disease-associated polyQ expansions preferentially form common structures that lead to toxicity (Perutz *et al.*, 1994; Tobin & Signer, 2000).

The antibody 3B5H10 binds preferentially to unaggregated mutant huntingtin and to several other proteins containing disease-associated polyQ expansions (Brooks *et al.*, 2004). Thus, 3B5H10 might bind to a putative structure shared by toxic forms of proteins with polyQ expansions. To define the structure of the paratope and gain insight into the mechanism of binding to polyQ expansions, we crystallized the Fab fragment of 3B5H10. Here, we describe the crystallization conditions, their optimization and preliminary X-ray studies of the crystals.

### 2. Material and methods

#### 2.1. Protein expression and purification

Monoclonal antibody (mAb) 3B5H10 was raised against a fusion protein encoding glutathione-*S*-transferase fused at its carboxyl terminus to an amino-terminal 171-amino-acid fragment of huntingtin containing a stretch of 66 glutamines (GST-htt 171-66Q), as described in Brooks *et al.* (2004). Large-scale production of 3B5H10 was carried out at the National Cell Culture Center using a 3B5H10 hybridoma line grown in Hyclone serum-free medium. The 3B5H10 Fab was prepared and purified as described by Brooks *et al.*



© 2005 International Union of Crystallography  
All rights reserved

**Table 1**

Comparison of the 3B5H10 crystal forms.

Values in parentheses are for the last resolution shell.

	Original	+ Ethyl acetate	+ Ethyl acetate + dehydration
Resolution (Å)	30.0–2.2 (2.52–2.50)	30.0–2.2 (2.65–2.60)	15–1.9 (2.00–1.90)
Maximum resolution of the weak wedge (Å)	3.0	2.5	2.0
Wavelength (Å)	0.900	0.826	1.078
Space group	$P2_12_12$	$P2_12_12$	$P2_1$
Unit-cell parameters			
$a$ (Å)	133.3	133.3	123.6
$b$ (Å)	78.54	79.52	78.25
$c$ (Å)	41.36	41.49	42.26
$\beta$ (°)	90	90	90.3
Average mosaicity (°)	0.9	0.4	0.4
Mosaicity of weak wedge (°)	1.2	0.9	0.5
Completeness (%)	100 (94.4)	99.5 (62.5)	95.6 (79.7)
Redundancy	8.9 (6.2)	13.5 (8.97)	3.2 (1.6)
$\langle I/\sigma(I) \rangle^\dagger$	44.3 (10.7)	39.2 (11.0)	10.8 (5.2)
$R_{\text{sym}}^\ddagger$	4.2 (15.3)	5.4 (22.1)	8.1 (23.6)
Matthews coefficient (Å <sup>3</sup> Da <sup>-1</sup> )	2.19	2.22	2.06
Molecules in asymmetric unit	1	1	2
Solvent content (%)	43	44	40

$^\dagger \langle I/\sigma(I) \rangle = \sum_i I_i/\sigma(I_i)$ .  $^\ddagger R_{\text{sym}} = \sum_{ij} |I_{i,j} - \langle I_i \rangle| / \sum_{ij} I_{i,j}$ , where  $I_{i,j}$  is the intensity of the  $j$ th observation of the  $i$ th reflection and  $\langle I_i \rangle$  is the average intensity of the  $i$ th reflection.

(2004) with minor modifications. The molecular mass of the 3B5H10 Fab is 46.75 kDa as determined by mass spectrometry.

## 2.2. Crystallization

Crystallization conditions were tested by the vapor-diffusion method using hanging drops suspended over 24-well Linbro tissue-culture plates. With the Low Ionic Screen (Hampton Research), drops composed of 4  $\mu$ l 3B5H10 (5 mg ml<sup>-1</sup>) in 5 mM Tris pH 8.0, 2  $\mu$ l buffer and 5  $\mu$ l 8, 16 or 24% (w/v) PEG 3350 were equilibrated over a 24% (w/v) PEG 3350 reservoir. Large feathery crystals appeared within three weeks in the 24% (w/v) PEG 3350 and 100 mM citric acid pH 4.5 condition.

Streak-seeding from a crushed crystal was used to nucleate crystal growth in pre-equilibrated drops. The seeded drops were typically composed as above. The protein concentration of 3B5H10 Fab was 3–5 mg ml<sup>-1</sup>, the citric acid buffer concentration was 10–200 mM and the pH was 4.5–5.0. The concentration of PEG 3350 in the well was held constant at 24% (w/v). The time for pre-equilibration was 8–48 h.

PEG 3350 was from Hampton Research. All other chemicals were from Fluka. The pH of buffers was adjusted before combination with PEG 3350. All drops were allowed to equilibrate at 297 K.

An additive search was conducted with Additive Screens 1, 2 and 3 (Hampton Research) and the optimized seeding conditions. Additive solutions were added to the drops in ratios of 1  $\mu$ l additive to 9  $\mu$ l drop volume. Over 20 different additives resulted in crystal formation after one week.

## 2.3. Cryoprotection

Crystals were washed with solutions containing 24–35% (w/v) PEG 3350, 20 mM citric acid pH 5.0 and 10–30% (v/v) cryoprotectant (Cryopro Kit, Hampton Research). Crystals were cryocooled by rapid immersion in liquid nitrogen or by direct placement into the cryostream.

## 2.4. Dehydration

Crystals were treated with cryoprotectant and mounted in Hampton 20  $\mu$ m loops. The crystals were dehydrated by touching a dental wick to the stem of the loop to remove excess mother liquor followed by exposure to room air for 20–60 s prior to flash-cooling in liquid nitrogen.

## 2.5. Data collection and processing

Room-temperature data were collected with a Rigaku R-AXIS IV image plate and an HR3 rotating-anode generator (50 keV, 100 mA) with Yale mirrors. Synchrotron data were collected at beamline 9-1 at Stanford Synchrotron Radiation Laboratory and beamlines 8.2.1, 8.2.2 and 8.3.1 at the Advanced Light Source. Data were processed and scaled with either *DENZO/SCALEPACK* (Otwinowski & Minor, 1997) or *XDS/XSCALE* (Kabsch, 1993).

## 3. Results and discussion

3B5H10 Fab formed large single crystals after streak-seeding into drops composed of 4  $\mu$ l 1.9 mg ml<sup>-1</sup> 3B5H10 Fab, 2  $\mu$ l 200 mM citric acid pH 4.5 and 5  $\mu$ l 22% (w/v) PEG 3350 equilibrated over 24% (w/v) PEG 3350 for 48 h (Fig. 1). These crystals diffracted to 1.7 Å at room temperature (~297 K) with X-rays from a rotating-anode source. A survey of five crystals indicated that the diffraction patterns were anisotropic with a weak zone of sharply decreased resolution (2.5 Å). The crystals also had a relatively high degree of mosaicity (>1.0°). In

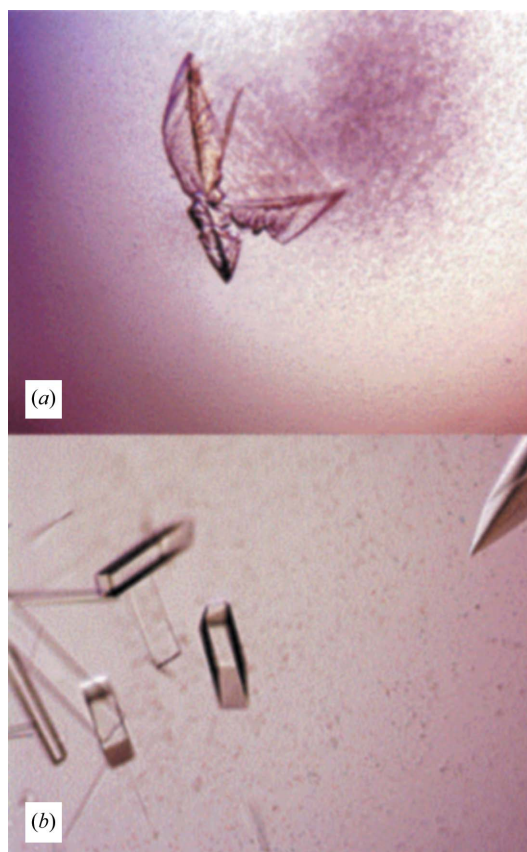


**Figure 1**  
(a) Crystals of 3B5H10 Fab that grew spontaneously from 24% PEG 3350 and 22 mM citric acid pH 4.5. (b) Crystals of 3B5H10 Fab after streak-seeding into 12% PEG 3350 and 22 mM citric acid pH 5.0. The drops were pre-equilibrated over 24% PEG 3350 for 48 h. The longest typical crystal dimension was 0.1–0.3 mm.

addition, the resolution of the diffraction pattern started decaying within 6 h of exposure, indicating that these crystals were also radiation-sensitive.

Since collecting diffraction data at cryogenic temperatures decreases the sensitivity of protein crystals to radiation damage, we determined the optimal cryoprotectant and cooling method for the 3B5H10 Fab crystals. After numerous trials with 25 cryoprotectants, we found that the crystals could be cryoprotected by a brief soak (<30 s) in 5%(v/v) ethylene glycol, 28%(w/v) PEG 3350 and 20 mM citric acid pH 5.0. The maximal resolution of the ethylene glycol-treated crystals at ~100 K was 2.2 Å in the strongest part of the pattern and 2.7–3.2 Å in the weakest (Table 1). The diffraction quality did not differ whether the crystals were cryocooled by rapid immersion in liquid nitrogen or by placement into the cryostream.

Although ethylene glycol treatment reduced the radiation sensitivity and enabled us to collect complete low-temperature data sets, the diffraction pattern was still anisotropic and of much lower quality than that of crystals mounted in a capillary at room temperature. During the cryoprotection search, we found that smaller crystals (longest axis <0.2 mm) tended to give a less anisotropic diffraction pattern than large crystals and that the diffraction quality was generally better in a region near the center of the crystal. These observations are consistent with the possibility that anisotropic diffraction patterns resulted from lattice deformation induced by mechanical or osmotic stress. Attempts to minimize stress by growing crystals in the presence of the cryoprotectant or passing them through solutions with increasing cryoprotectant concentrations did not reduce the anisotropy.

Therefore, we decided to look for a second crystal form that was more resistant to stress. A series of additives was tested with Hampton Additive Screens 1, 2 and 3 and the original crystallization condition. More than 20 of the 72 additives gave diffraction-quality crystals. Most of the additives delayed crystal growth by 6–15 d but

had little effect or decreased the diffraction limit. Three additives (betaine monohydrate, ATP and ethyl acetate) reduced both the mosaicity of the crystals and the anisotropy of the diffraction pattern, suggesting greater resistance to stress. All of these crystals were morphologically identical to the original crystals. The most effective additive, ethyl acetate, delayed crystal growth by 5–7 d and increased the resolution of the weak wedge in the diffraction pattern from 3.0 to 2.5 Å and decreased the average mosaicity from 0.9 to 0.4° (Table 1). Crystals grown using the optimized concentration of ethyl acetate, 5%(v/v), are shown in Fig. 1(b).

In combination with ethyl acetate, dehydration dramatically increased the resolution of the diffraction pattern to limits similar to those of the crystals at room temperature. The resolution was 1.7 Å in the strong part of the diffraction pattern and 2.0 Å in the weak part. The mosaicity calculated from the reflections in the weak part improved from 0.9 to 0.5°, which suggested that the dehydrated crystals had better long-range order.

The method of dehydration was critical. The 3B5H10 crystals were dehydrated by exposing the mounted crystals to room air after removal of the excess cryoprotectant and before immersion in liquid nitrogen. This method is relatively harsh and difficult to replicate. However, controlled dehydration methods such as adding variable amounts of 100% PEG 3350 to wells containing mature crystals or equilibration of mature drops over concentrated salts (Tahirov *et al.*, 1998) failed because the 3B5H10 Fab crystals dissolved over a period of hours.

Dehydration changed the apparent space group of the 3B5H10 crystals from  $P2_12_12$  to  $P2_1$ . The self-rotation function calculated from data collected from the dehydrated crystal shows that the twofold axes in the orthorhombic cell are preserved in the  $P2_1$  cell but are slightly shifted (Fig. 2). Inspection of the orthorhombic crystals showed that all of the expected systematic absences along the  $h00$  and  $k00$  axes above  $h = 5$  and  $k = 5$  had an  $(I/\sigma(I))$  of 2.5–3.5, consistent with the presence of deviations from the crystallographic symmetry within the orthorhombic crystals. However, these deviations must be quite small since, as will be presented in a subsequent publication, the structure of the 3B5H10 Fab in the orthorhombic crystal form has been solved using SIRAS.

#### 4. Summary

Although the 3B5H10 Fab crystallized readily into large single crystals, extensive optimization was required to obtain an isotropic diffraction pattern suitable for structure solution. Mechanical or osmotic stress during handling appeared to be the source of the anisotropy, although defects incorporated into the lattice during rapid growth of the crystals cannot be ruled out. Adding ethyl acetate to the crystallization buffer slowed the growth rate and resulted in crystals that survived the relatively harsh dehydration conditions. Dehydration improved the quality of the diffraction pattern and increased the diffraction limit of the cryocooled crystals to that of the capillary-mounted room-temperature crystals.

We thank Chad A. Sinkler and Mike Welch (National Cell Culture Center) and Shing-Erh Yen (Zymed) for the special care they gave to this project, Stephen Ordway and Gary Howard for editorial assistance and Kelley Nelson for administrative assistance. This work was supported by the High Q Foundation, a Therapeutics Initiative Award from the Huntington's Disease Society of America and the National Institute of Aging (P01 AG022074). Additional support was provided by the National Institute of Neurological Disease and

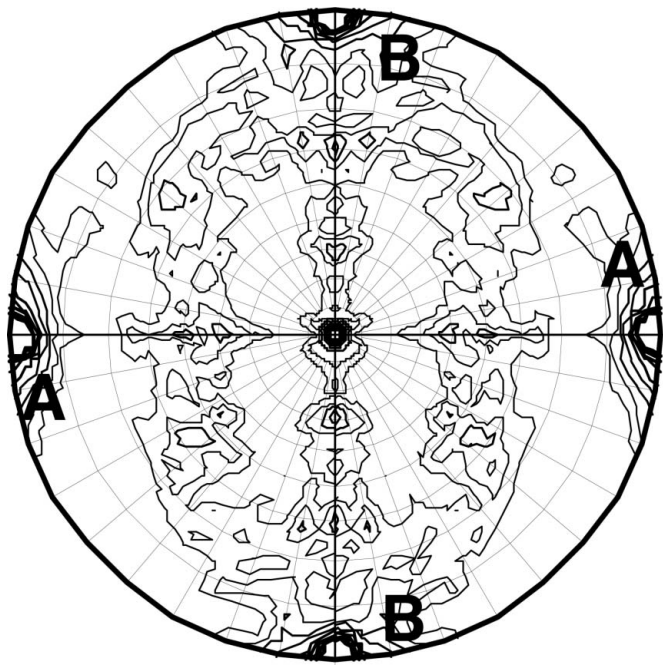


**Figure 2**  
 $\kappa = 180^\circ$  self-rotation function for the dehydrated ethyl acetate-treated crystals plotted in polar angles showing pseudo-222 symmetry. The longitude lines represent  $\theta$  and the latitude lines represent  $\varphi$ . The crystallographic twofold is the sharp peak at (0, 0). Peaks A (0,  $90^\circ$ ) and B ( $90^\circ$ ,  $90^\circ$ ) are the noncrystallographic twofolds.

Stroke (R01 NS39074) and the Taube Family Foundation Program in Huntington's Disease. Antibody production was carried out at the National Cell Culture Center with the support of the National Institutes of Health, National Center for Research Resources. Portions of this research were carried out through the general user programs at the Stanford Synchrotron Radiation Laboratory and the Advanced Light Source.

### References

- Arrasate, M., Mitra, S., Schweitzer, E. S., Segal, M. R. & Finkbeiner, S. (2004). *Nature (London)*, **431**, 805–810.
- Brooks, E., Arrasate, M., Cheung, K. & Finkbeiner, S. (2004). *Methods Mol. Biol.* **277**, 103–128.
- Davies, S. W., Turmaine, M., Cozens, B. A., DiFiglia, M., Sharp, A. H., Ross, C. A., Scherzinger, E., Wanker, E. E., Mangiarini, L. & Bates, G. P. (1997). *Cell*, **90**, 537–548.
- Kabsch, W. (1993). *J. Appl. Cryst.* **26**, 795–800.
- Klement, I. A., Skinner, P. J., Kaytor, M. D., Yi, H., Hersch, S. M., Clark, H. B., Zoghbi, H. Y. & Orr, H. T. (1998). *Cell*, **95**, 41–53.
- MacDonald, M. E. (1998). *Results Probl. Cell Differ.* **21**, 47–75.
- Otwinowski, Z. & Minor, W. (1997). *Methods Enzymol.* **276**, 307–326.
- Perutz, M. F., Johnson, T., Suzuki, M. & Finch, J. T. (1994). *Proc. Natl Acad. Sci. USA*, **91**, 5355–5358.
- Saudou, F., Finkbeiner, S., Devys, D. & Greenberg, M. E. (1998). *Cell*, **95**, 55–66.
- Scherzinger, E., Sittler, A., Schweiger, K., Heiser, V., Lurz, R., Hasenbank, R., Bates, G. P., Lehrach, H. & Wanker, E. E. (1999). *Proc. Natl Acad. Sci. USA*, **96**, 4604–4609.
- Tahirov, T. H., Oki, H., Tsukihara, T., Ogasahara, K., Yutani, K., Libeu, C. P., Izu, Y., Tsunasawa, S. & Kato, I. (1998). *J. Struct. Biol.* **121**, 68–72.
- Tobin, A. J. & Signer, E. R. (2000). *Trends Cell Biol.* **10**, 531–536.
- Zoghbi, H. Y. & Orr, H. T. (2000). *Annu. Rev. Neurosci.* **23**, 217–247.